bioRxiv preprint doi: https://doi.org/10.1101/051912; this version posted May 6, 2016. The copyright holder for this preprint (which was not certified by peer review) is the author/funder, who has granted bioRxiv a license to display the preprint in perpetuity. It is made available under aCC-BY-NC-ND 4.0 International license.

High-yield methods for accurate two-alternative visual psychophysics in head-fixed mice

Christopher P Burgess[1], Nicholas Steinmetz[2], Armin Lak[1], Peter Zatka-Haas[2,3], Adam Ranson[1], Miles Wells[2], Sylvia Schröder[1], Elina A K Jacobs[2], Charu Bai Reddy[1], Sofia Soares[4], Jennifer F Linden[5], Joseph J Paton[4], Kenneth D Harris[2], Matteo Carandini[1]*

1, UCL Institute of Ophthalmology, University College London, London EC1V 9EL, United Kingdom

2, UCL Institute of Neurology, University College London, London WC1E 6DE, United Kingdom

3, Centre for Mathematics and Physics in the Life Sciences and Experimental Biology (CoMPLEX), University College London, United Kingdom

4, Champalimaud Centre for the Unknown, Lisbon, Portugal

5, UCL Ear Institute, University College London, London WC1X 8EE, United Kingdom

[*]Present address: Neurosciences & Mental Health Research Institute, Cardiff University School of Medicine, Cardiff CF24 4HQ, United Kingdom

Abstract

Research in neuroscience relies increasingly on the mouse, a mammalian species that affords unparalleled genetic tractability and brain atlases. Here we introduce high-yield methods for probing mouse visual decisions. Mice are head-fixed, which facilitates repeatable visual stimulation, eye tracking, and brain access. They turn a steering wheel to make two-alternative choices, forced or unforced. Learning is rapid thanks to intuitive coupling of stimuli to wheel position. The mouse decisions deliver high-quality psychometric curves for detection and discrimination, and conform to the predictions of a simple probabilistic observer model. The task is readily paired with two-photon imaging of cortical activity. Optogenetic inactivation reveals that the task requires the visual cortex. Mice are motivated to perform the task by fluid reward or optogenetic stimulation of dopaminergic neurons. This stimulation elicits larger number of trials and faster learning. These methods provide a platform to accurately probe mouse vision and its neural basis.

Introduction

The mouse is increasingly the species of choice for experiments that seek to understand the mammalian brain. Its advantages in ease of husbandry, breeding, and handling have been recognized for over 100 years, with the establishment of inbred lines that allowed researchers to control for genetic variation[1]. Today the mouse offers an unrivaled arsenal of tools to the neuroscientist, from atlases of gene expression[2] and connectivity[3,4] to a vast array of genetic tools [5] and transgenic lines[6-9]. An additional advantage of the mouse is that its cortex is not folded, so it is more accessible to imaging studies.

Mice are also an excellent species for probing mechanisms of visual perception, decision, and cognition. Mice are readily trained to perform behavioral tasks based on touch[10] or on vision[11]. Tasks based on vision, specifically, have been extended to probe not only sensation and perception, but also aspects of cognition[12,13].

Contrary to past preconceptions, mice make major use of vision[14,15]. The mouse visual cortex comprises a network of at least 12 retinotopic areas[16,17]. These areas might not map one-to-one to the 16-30 visual areas found in primates[18-20], but the principles governing the division of labor across areas are likely to be conserved across species. These and other principles of visual brain function may be fruitfully investigated in the mouse.

Studying the neural activity underlying visually-driven behavior, however, requires careful psychophysical techniques that pose specific constraints[15]. First, one must precisely control visual stimulation and be able to measure eye

bioRxiv preprint doi: https://doi.org/10.1101/051912; this version posted May 6, 2016. The copyright holder for this preprint (which was not certified by peer review) is the author/funder, who has granted bioRxiv a license to display the preprint in perpetuity. It is made available under aCC-BY-NC-ND 4.0 International license.

position. Second, one must be able to pair psychophysics with brain recordings or manipulations. Third, the task should be robust to changes in the observer's overall tendency to respond. Fourth, the task should be learned quickly and reliably by most subjects. Fifth, the task should yield many trials per stimulus and per session, to deliver precise psychometric curves relating task performance to visibility. Sixth, the task should yield close to 100% performance on easy trials, to distinguish errors due to the limits of vision from those that result from other sources (disengagement, confusion about the task rules, errors in motor control). Seventh, it would be ideal if one could motivate the subject to perform the task without limitations in food or water availability. Finally, the task should be flexible, so that its design can be made more complex if needed.

These fundamental requirements are not met by the existing techniques for mouse visual psychophysics. The first two requirements – careful control of visual stimulation and ability to perform brain recordings and manipulations – strongly argue in favor of head fixing, as some forms of brain recording or imaging can only be performed in an immobile brain. This requirement rules out techniques based on swimming[21] or on poking the nose[12,13,22,23]. Some existing techniques available to study vision are compatible with head fixing, but they probe hard-wired behavior such as the optokinetic reflex[24], which does not require higher brain centers such as visual cortex. The third requirement – robustness to the observer's tendency to respond – strongly argues for having the observer choose between two stimuli[15] (two-alternative choice). This rules out techniques where the mouse report the presence or absence of a visual stimulus (go/no-go) by licking a single spout[11,25,26]. Methods for two-alternative choices have been developed to probe audition[27], somatosensation[10], and olfaction[28], but it is not known if these work to probe vision. Finally, no existing techniques meet the ideal requirement of a positive reward with no implicit punishment. In current tasks, the reward is a partial redressing of an unpleasant condition, be it immersion in water[21], or a sensation of thirst[11-13,22,23,25,26].

We thus developed a new task that meets all the above requirements. In the task, head-fixed mice turn a steering wheel left or right to provide a two-alternative choice between visual stimuli. Mice learn this task quickly thanks to intuitive coupling of the steering wheel to the position of the visual stimuli. They learn it whether the reward is water or selective stimulation of midbrain dopaminergic neurons. Mice perform the task proficiently, and their decisions conform to the predictions of a simple probabilistic observer model. The task can be readily paired with two-photon imaging, activates visual cortex, requires visual cortex, and can be flexibly extended to probe unforced-choice, both for stimulus detection and for stimulus discrimination.

Results

We begin by introducing the basic design of the task: two-alternative forced-choice contrast detection with a water reward, and we show that this task is compatible with precise recordings of visual responses in cortex. We then introduce the unforced-choice version of the task, we define a simple probabilistic observer model for the mouse decisions, and we show how these decisions are impaired by inactivation of visual cortex. Finally, we illustrate two variations of the method: one where the reward is optogenetic stimulation of dopaminergic neurons rather than water, and one where the task involves discrimination between two stimuli in opposite visual fields.

The basic task: two alternative forced-choice (2AFC)

To allow a head-fixed mouse to select one of two choices, we placed a steering wheel under the front paws, and coupled its position to the position of a visual stimulus on the screen (Figure 1**a**,**b**). We chose the wheel as manipulandum (Figure 1**a**) as it resembles those successfully used to probe mouse audition [27] and mouse olfaction [28]. To train mice to use this manipulandum in a visual task, it was highly advantageous to couple wheel movements to the visual stimuli, so that turning the wheel left or right would accordingly move the stimuli left or right (Figure 1**b**; Supplementary Movie 1). The mouse indicates its choice of stimulus by bringing that stimulus to the center of the visual field.

bioRxiv preprint doi: https://doi.org/10.1101/051912; this version posted May 6, 2016. The copyright holder for this preprint (which was not certified by peer review) is the author/funder, who has granted bioRxiv a license to display the preprint in perpetuity. It is made available under aCC-BY-NC-ND 4.0 International license.

The typical sequence of trial events was as follows (Supplementary Figure 1**a**)**.** First, the mouse had to keep the wheel still to initiate the trial and make the stimulus appear. Second, if needed in the experiment (e.g. during imaging) an "open loop" period began during which wheel movements were ignored. Mice generally continued to hold the wheel still in this period, and if the experiment required this behavior, it was reinforced through training. Third, a tone was typically played, after which the mouse could respond at any time, and wheel turns resulted in movements of the visual stimuli ("closed loop", Figure 1**b**). The reward for a correct decision was a small amount of water (1-3 µL, typically adjusted by body weight). An incorrect decision was penalized with a 2 s timeout signaled by a noise burst.

Training for a typical mouse proceeded in two main stages (Figure 1**c**-**e**). We started the mouse on easy (high) contrasts, until it learned the association between turning the wheel and moving the stimulus, and receiving rewards. When the mouse was above chance level performance (typically, by the first week), we began to introduce lower contrasts. For example, a typical mouse (Figure 1**c**) reached 56% performance on a high contrast stimulus after ~2,300 trials (Figure 1**d***, blue*), on day 5 (Figure 1**e***, blue*), after which we introduced lower contrast stimuli. High-quality psychometric functions of stimulus contrast and position were obtained by week three (Figure 1**c**). By week four, this animal had mastered the task.

These results were typical of our population (n = 98 mice, Figure 1**d**-**g**). Most mice were above chance before ~1,000 trials (Figure 1**d**), corresponding to a few days of training (Figure 1**e**). Mice then typically approached steady performance after ~7,000 trials (Figure 1**d**). In this early period, mice typically performed 100-300 trials per day, so this performance was typically obtained in little over 20 training days (Figure 1**e**). Most animals surpassed 80% performance, but a sizeable fraction (38/98) also reached 90% performance (Figure 1**g**). Only few mice (6/98) failed to learn the task by trial 5,000 or after two weeks (Figure 1**f**,**g**).

Once they mastered the task, mice typically produced consistent movements, with initial wheel deflections usually matching the final responses made (Supplementary Figure 2). If desired, we could then modify the task by removing the coupling between wheel position and stimulus position, so that the stimulus would stay fixed in its position (Supplementary Figure 3), or disappear as soon as the movement started.

Simultaneous recordings in visual cortex

To confirm that this task could be readily paired with measurements of brain activity, we performed two-photon imaging of activity in primary visual cortex (V1) of mice that were performing the task (Figure 2). We expressed GCaMP6m in V1 neurons (right hemisphere) via AAV2/1 virus injection, and trained the mice in a version of the task where the "open loop" period lasted 1 s (Supplementary Figure 1**a**). During this period we could image neural responses without the stimulus moving. While mice performed this task (Figure 2**a**) we performed two-photon calcium imaging of V1 neurons, choosing a field of view with cells whose receptive field overlapped with the (contralateral) stimulus (Figure 2**b**).

As expected, most visually-responsive cells showed robust responses to contralateral stimuli, and gave no response to ipsilateral stimuli (Figure 2**c**-**d**). The onset of contralateral stimuli evoked strong calcium transients during the open loop period (Figure 2**c**). The amplitudes of these transients grew with the contrast c of contralateral gratings (Figure 2**d**). We fit these responses with the commonly used function[29,30]

$$f(c) = \frac{c^n}{c_{50}^n + c^n} \qquad (1)$$

where c_{50} and n are free parameters. Similar results were routinely obtained in other mice (e.g. Figure 2**e**-**h**). These results demonstrate that the visual task can be readily paired with recording techniques that require high stability, and that it evokes reliable activity in cortex.

bioRxiv preprint doi: https://doi.org/10.1101/051912; this version posted May 6, 2016. The copyright holder for this preprint (which was not certified by peer review) is the author/funder, who has granted bioRxiv a license to display the preprint in perpetuity. It is made available under aCC-BY-NC-ND 4.0 International license.

Two alternative unforced-choice (2AUC)

In many conditions, it helps to extend a two-alternative task by allowing a "no-go" response option when the stimulus is absent. With this two-alternative unforced choice (2AUC) version of the task, one can measure sensitivity and bias separately for the two stimulus locations. This is particularly useful following unilateral manipulations in task context or brain activity[31].

We found that mice were readily able to learn this 2AUC task (Figure 3**a**,**b**). After training mice on the 2AFC task, we added the no-go condition: when the stimulus was absent (zero contrast), mice would earn the reward by refraining from turning the wheel (no-go, Figure 3**a**) for the duration of a 1.5 second response window (Figure 3**b**). Mice readily learned this new response contingency (Figure 3**b**). Their reaction times for responses left or right were much faster than the 1.5 s response window (Supplementary Figure 1**b**), indicating that issuing a no-go response was distinct from simply being slow to respond. Consistent with this interpretation, mice made most no-go choices at zero contrast (when these choices were correct), and made progressively fewer of them as stimulus contrast increased (Figure 3**b**).

Probabilistic observer model

The decisions made by the mice in the task conformed closely to the predictions of a simple probabilistic observer model. We present here the model for the 2AUC version of the task, as this is the more general case (Figure 3**c**,**d**). The model outputs the probability to choose left p_L or right p_R relative to the probability of choosing no-go p_0. The log odds of choosing left or right vs. choosing no-go are given by two decision variables z_L and z_R, which in turn depend on the contrast on the left c_L and on the right c_R:

$$\log\left(\frac{p_L}{p_0}\right) = z_L \coloneqq b_L + s_L f(c_L) \qquad (2)$$

$$\log\left(\frac{p_R}{p_0}\right) = z_R \coloneqq b_R + s_R f(c_R)$$

These two expressions fully describe the three probabilities because by definition $p_R + p_L + p_0 = 1$. In these expressions, the parameters b_L and b_R measure the bias to choose left or right relative to choosing no-go, the parameters s_L and s_R measure the weight assigned to sensory evidence on the left or right, and $f(c)$ is the function of contrast in Equation 1 (Figure 3**c**). We fit the 4 parameters of this decision model through multinomial logistic regression and optimized the additional two parameters describing contrast sensitivity (Equation 1). With 6 parameters, the model provided excellent fits to the 22 measurements (curves in Figure 3**b**).

Inactivation in visual cortex

To assess the involvement of visual cortex in task performance, we employed optogenetic techniques to inactivate cortical areas during individual trials. We used transgenic mice expressing ChR2 in *Pvalb*-positive inhibitory interneurons and implanted them with clear skull caps [32]. A 473 nm laser was used to unilaterally inactivate the visual cortex or control sites in somatosensory cortex (Figure 4**a**) during visual stimulus presentation and wheel-turn responses (Supplementary Figure 3**c**). Electrophysiological measurements show that such inactivation was circumscribed to a radius of ~1 mm (Supplementary Figure 4).

Inactivation of visual cortex strongly suppressed the mouse's ability to detect contralateral stimuli (Figure 4**b**,**c**). Inactivating left visual cortex had barely any effect on the detection of ipsilateral stimuli, but greatly increased the fraction of no-go responses to contralateral stimuli, and correspondingly decreased the correct detection of those stimuli (Figure 4**b**). Analogous results were seen when inactivating right visual cortex (Figure 4**c**).

To summarize these effects and compare them across experiments, we used the probabilistic observer model (Figure 4**d**-**f**). In the example experiment, inactivation of left visual cortex reduced only the decision variable for right stimuli

bioRxiv preprint doi: https://doi.org/10.1101/051912; this version posted May 6, 2016. The copyright holder for this preprint (which was not certified by peer review) is the author/funder, who has granted bioRxiv a license to display the preprint in perpetuity. It is made available under aCC-BY-NC-ND 4.0 International license.

(z_R, Figure 4**d**), and inactivation of right visual cortex reduced only the decision variable for left stimuli (z_L, Figure 4**e**). Similar results were seen across experiments (Figure 4**f**): inactivation of left visual cortex decreased z_R by 2.9±0.1, significantly more than z_L (1.0±0.2; paired t-test $p<10^{-5}$), and inactivation of right visual cortex decreased z_L by 2.0±0.2, significantly more than z_R (0.5±0.2; $p<10^{-4}$).

We conclude that accurate performance on this task requires that mice make use of their visual cortex. This requirement, moreover, is specific to visual cortex: inactivation of somatosensory cortex did not cause any lateralized change in decision variables (p=0.17 and p=0.25 for inactivation of left and right somatosensory cortex).

Rewarding with optogenetic dopamine stimulation

The conventional method to reward mice for performing perceptual decisions involves delivering fluids under conditions of water control [10-13,15,22,23,25,26]. We sought to improve on this by providing direct stimulation of the brain centers that mediate the effects of positive reinforcement. This method would not require water or food restriction.

To motivate the animals to learn and perform the task, we provided phasic optogenetic stimulation of midbrain dopamine (DA) neurons. Phasic stimulation of these neurons, delivered electrically[33] or optogenetically[34], has long been known to be sufficient for behavioral conditioning We injected a viral construct containing Cre-dependent Channelrhodopsin-2 (ChR2) into ventral tegmental area (VTA) and substantia nigra pars compacta (SNc) of $DAT^{IREScre}$ mice, and we implanted an optic fiber above VTA (Figure 5**a**).

We confirmed specific expression of ChR2 in dopamine neurons using immunohistochemistry (Figure 5**b**). We identified dopaminergic neurons as those that stained for tyrosine hydroxylase (TH+). Over 77% of them also expressed ChR2. On the other hand, less than 3% of neurons that expressed ChR2 failed to react to TH staining, indicating that the expression was highly selective to DA neurons.

We then trained the naïve mice in our 2AFC task and reinforced correct choices with only optogenetic dopamine stimulation and an associated sound. In this preparation, a correct wheel response was followed by a click sound and a simultaneous short train (~ 0.5 s) of laser pulses. The mice did not receive a water reward, and had free access to food and water in their home cage.

Mice trained with optogenetic DA stimulation rapidly learned the task, greatly outperforming mice trained for a water reward, both in speed of learning and in number of trials per session (Figure 5**c**-**f**). After only a few days of training with DA stimulation, mice often performed over 1,000 trials per session, with high accuracy (Figure 5**c**-**d**), resulting in high-quality psychometric curves (Figure 5**e**). On average, mice rewarded with DA stimulation performed almost twice as many trials per session as those that were rewarded with water (Figure 5**f**).

Stimulus discrimination

An important feature of a method for performing psychophysics is that it must be flexible, so that its design can be altered or made more complex as needed. For instance, the basic tasks that we have described, whether 2AFC or 2AUC, involve detecting whether a stimulus appears on the left or right side. To study mechanisms that combine information across hemispheres, however, it is useful to have the subject discriminate between stimuli that appear on both sides, as in contrast discrimination tasks that are commonly used with human observers[35-37].

Mice that had already learned the 2AUC detection task readily learned to perform a more general contrast discrimination task (Figure 6). In most trials, two stimuli appeared on the screen, and the mice were rewarded with water for selecting the stimulus that had the higher visual contrast (Figure 6**a**). A no-go response was rewarded when no grating was presented on either side. Mice quickly learned this generalization of the task, yielding high-quality psychometric curves (Figure 6**b**). When one of the gratings had zero contrast (a "pedestal contrast" of 0%, Ref. 37) the task was equivalent to contrast detection (e.g. Figure 3). When both gratings were present the mouse correctly gave fewer no-go responses, while finding it harder to indicate the side with higher contrast. Similar results

bioRxiv preprint doi: https://doi.org/10.1101/051912; this version posted May 6, 2016. The copyright holder for this preprint (which was not certified by peer review) is the author/funder, who has granted bioRxiv a license to display the preprint in perpetuity. It is made available under aCC-BY-NC-ND 4.0 International license.

were seen in all three mice (Figure 6**b**-**d**). Mouse decisions conformed closely to the predictions of the probabilistic observer model that we had introduced for contrast detection (Figure 3). With a fixed setting of its 6 parameters the model provided satisfactory fits to the 32 response probabilities measured across three pedestal contrasts.

These results illustrate the suitability of the task for studying sophisticated psychophysical paradigms. The task is flexible and can be modified in multiple ways, and it leads the mice to provide psychophysical curves that are not dissimilar in quality from those seen in primates and humans.

Discussion

We have outlined a flexible task paradigm for assessing visual decision-making in mice. In this task, the mouse is head-fixed, allowing careful control of visual stimulation and measurement of eye position, and easing simultaneous brain recordings or manipulations. The steering wheel allows mice to accurately report one of two alternative stimuli, and the task is readily extended to allow a no response option (no-go response). The task is learned quickly and reliably: most mice master it within a few weeks. The task yields a large number of trials within a single session, providing high-quality psychometric curves within individual sessions.

The decisions that mice make in this task conform closely to the predictions of a simple probabilistic observer model. The model's formulation in terms of multinomial logistic regression is closely related to an earlier formulation based on signal detection theory [31]. Both formulations are two-dimensional, because their responses depend on the combination of two orthogonal decision variables. As we have seen, this two-dimensional nature is essential to capture the effects of unilateral cortical inactivations. Models that account for multiple possible responses with a one-dimensional decision variable[38-40] would not account for those effects. Our formulation, moreover, has two advantages over the earlier one[31]. First, by recasting the model as a logistic regression it is easier to include other predictor variables (e.g. past history [22] or neural activity [41]). Second, having a functional dependence on stimulus contrast minimizes the number of free parameters.

We further demonstrated that transient optogenetic dopamine stimulation can substitute water reward. Transient dopamine stimulation had been shown to be sufficient to drive simple behavioral conditioning such as conditioned place preference[34]. Our results show that it is sufficient to motivate mice for making choices in a perceptual decision task. The combination of our task and dopamine stimulation may thus be useful for studying the effects of dopamine signals on perception and perceptual learning[42,43].

Dopamine stimulation offers an attractive alternative to water restriction. It greatly accelerates task acquisition and almost doubles daily trial counts. Both advantages can be important. For instance, a large number of trials is particularly useful when relating perceptual decisions to neural activity. Moreover, the method is arguably less disruptive of the mouse's normal behavior and physiology, as it does not involve restriction on water intake.

As currently implemented, however, our optogenetic method also carries some limitations. First, the method requires the use of DAT-Cre mice, which may not be feasible if Cre needs to be expressed in other cells for other experimental purposes. Second, the method requires implantation of optic fibers, which take up valuable space on the head of the mouse.

A key advantage of our behavioral task is that it is highly flexible, allowing for multiple extensions of the same basic design. We have modified the task depending on requirements, for example introducing a cue informing mice when to initiate their response, and a no-go response option to report stimulus absence. We exploited this no-go response in inactivation experiments, finding that inactivation of visual cortex diminished reports of contralateral stimuli but left ipsilateral reports unaffected. We also modified the task in a variant requiring contrast discrimination between two stimuli, generating high-quality psychometric functions that were modulated by contrast difference and by the level of the pedestal contrast. Further, we found that once trained, mice continue to perform if the stimulus position

bioRxiv preprint doi: https://doi.org/10.1101/051912; this version posted May 6, 2016. The copyright holder for this preprint (which was not certified by peer review) is the author/funder, who has granted bioRxiv a license to display the preprint in perpetuity. It is made available under aCC-BY-NC-ND 4.0 International license.

is fixed or is only transiently presented, which can be exploited to address concerns about stimulus movement being related to choice, or of presentation durations being controlled by the mouse.

We believe that the coupling of wheel movements to stimulus properties is a particularly useful learning aid, and is further generalizable. For instance, the task can be extended beyond the detection or discrimination of visual contrast. In preliminary results (not shown), we have trained mice to use the wheel to rotate a grating to a target orientation or to modulate the pitch of repetitively presented tones toward a target pitch.

Moreover, the continuous readout available from the steering wheel may provide further insight into the nature of behavior. We used the wheel to obtain binary or ternary reports, but the continuous readout may afford more sensitive behavioral assays, potentially probing factors such as motivation, confidence[44], response vigor, and vacillation[45]. These considerations suggest extensions of the task to a fully interactive, flexible, and accurate platform to probe mouse vision and visuomotor behavior and establish their neural basis.

Acknowledgments

This work was supported by Senior Investigator Awards from the Wellcome Trust (MC and KDH), and by a Medical Research Council Doctoral Training Award (CPB), a Human Frontiers Science Program Fellowship (NS), a Sir Henry Wellcome Fellowship (AL), a Marie Skłodowska-Curie Fellowship (SS), and a Wellcome Trust PhD Studentship (EJ). MC holds the GlaxoSmithKline / Fight for Sight Chair in Visual Neuroscience.

References

1 Beck, J. A. *et al.* Genealogies of mouse inbred strains. *Nature genetics* **24**, 23-25 (2000).
2 Lein, E. S. *et al.* Genome-wide atlas of gene expression in the adult mouse brain. *Nature* **445**, 168-176 (2007).
3 Oh, S. W. *et al.* A mesoscale connectome of the mouse brain. *Nature* **508**, 207-214 (2014).
4 Zingg, B. *et al.* Neural networks of the mouse neocortex. *Cell* **156**, 1096-1111 (2014).
5 Huang, Z. J. & Zeng, H. Genetic approaches to neural circuits in the mouse. *Annu Rev Neurosci* **36**, 183-215 (2013).
6 Madisen, L. *et al.* Transgenic mice for intersectional targeting of neural sensors and effectors with high specificity and performance. *Neuron* **85**, 942-958 (2015).
7 Madisen, L. *et al.* A toolbox of Cre-dependent optogenetic transgenic mice for light-induced activation and silencing. *Nat Neurosci* (2012).
8 Harris, J. A. *et al.* Anatomical characterization of Cre driver mice for neural circuit mapping and manipulation. *Front Neural Circuits* **8**, 76 (2014).
9 Heintz, N. & Gerfen, C. The Gene Expression Nervous System Atlas (GENSAT) Project. (NINDS Contracts N01NS02331 & HHSN271200723701C, The Rockefeller University (New York, NY).).
10 Guo, Z. V. *et al.* Procedures for behavioral experiments in head-fixed mice. *PLoS One* **9**, e88678 (2014).
11 Andermann, M. L., Kerlin, A. M. & Reid, R. C. Chronic cellular imaging of mouse visual cortex during operant behavior and passive viewing. *Front Cell Neurosci* **4**, 3 (2010).
12 Bussey, T. J. *et al.* New translational assays for preclinical modelling of cognition in schizophrenia: the touchscreen testing method for mice and rats. *Neuropharmacology* **62**, 1191-1203 (2012).
13 Nithianantharajah, J. *et al.* Bridging the translational divide: identical cognitive touchscreen testing in mice and humans carrying mutations in a disease-relevant homologous gene. *Scientific reports* **5**, 14613 (2015).
14 Huberman, A. D. & Niell, C. M. What can mice tell us about how vision works? *Trends Neurosci* **34**, 464-473 (2011).
15 Carandini, M. & Churchland, A. K. Probing perceptual decisions in rodents. *Nat Neurosci* **16**, 824-831 (2013).
16 Glickfeld, L. L., Reid, R. C. & Andermann, M. L. A mouse model of higher visual cortical function. *Curr Opin Neurobiol* **24C**, 28-33 (2014).
17 Garrett, M. E., Nauhaus, I., Marshel, J. H. & Callaway, E. M. Topography and areal organization of mouse visual cortex. *J Neurosci* **34**, 12587-12600 (2014).
18 Markov, N. T. *et al.* Anatomy of hierarchy: feedforward and feedback pathways in macaque visual cortex. *J Comp Neurol* **522**, 225-259 (2014).

bioRxiv preprint doi: https://doi.org/10.1101/051912; this version posted May 6, 2016. The copyright holder for this preprint (which was not certified by peer review) is the author/funder, who has granted bioRxiv a license to display the preprint in perpetuity. It is made available under aCC-BY-NC-ND 4.0 International license.

19 Wandell, B. A., Dumoulin, S. O. & Brewer, A. A. Visual field maps in human cortex. *Neuron* **56**, 366-383 (2007).

20 Felleman, D. J. & Van Essen, D. C. Distributed hierarchical processing in the primate cerebral cortex. *Cereb Cortex* **1**, 1-47 (1991).

21 Prusky, G. T., West, P. W. & Douglas, R. M. Behavioral assessment of visual acuity in mice and rats. *Vision Res* **40**, 2201-2209 (2000).

22 Busse, L. *et al.* The detection of visual contrast in the behaving mouse. *J Neurosci* **31**, 11351-11361 (2011).

23 Long, M., Jiang, W., Liu, D. & Yao, H. Contrast-dependent orientation discrimination in the mouse. *Scientific reports* **5**, 15830 (2015).

24 Cahill, H. & Nathans, J. The optokinetic reflex as a tool for quantitative analyses of nervous system function in mice: application to genetic and drug-induced variation. *PLoS One* **3**, e2055 (2008).

25 Glickfeld, L. L., Histed, M. H. & Maunsell, J. H. Mouse primary visual cortex is used to detect both orientation and contrast changes. *J Neurosci* **33**, 19416-19422 (2013).

26 Lee, S. H. *et al.* Activation of specific interneurons improves V1 feature selectivity and visual perception. *Nature* **488**, 379-383 (2012).

27 Sanders, J. & Kepecs, A. Choice Ball: a response interface for psychometric discrimination in head-fixed mice. *J Neurophysiol* (2012).

28 Resulaj, A. & Rinberg, D. Novel Behavioral Paradigm Reveals Lower Temporal Limits on Mouse Olfactory Decisions. *J Neurosci* **35**, 11667-11673 (2015).

29 Albrecht, D. G. & Hamilton, D. B. Striate cortex of monkey and cat: contrast response function. *J. Neurophysiol.* **48**, 217-237 (1982).

30 Sclar, G., Maunsell, J. H. & Lennie, P. Coding of image contrast in central visual pathways of the macaque monkey. *Vision Res* **30**, 1-10 (1990).

31 Sridharan, D., Steinmetz, N. A., Moore, T. & Knudsen, E. I. Distinguishing bias from sensitivity effects in multialternative detection tasks. *J Vis* **14** (2014).

32 Guo, Z. V. *et al.* Flow of cortical activity underlying a tactile decision in mice. *Neuron* **81**, 179-194 (2014).

33 Olds, J. & Milner, P. Positive reinforcement produced by electrical stimulation of septal area and other regions of rat brain. *Journal of comparative and physiological psychology* **47**, 419-427 (1954).

34 Tsai, H. C. *et al.* Phasic firing in dopaminergic neurons is sufficient for behavioral conditioning. *Science* **324**, 1080-1084 (2009).

35 Nachmias, J. & Sansbury, R. V. Grating contrast: discrimination may be better than detection. *Vision Res* **14**, 1039-1042 (1974).

36 Boynton, G. M., Demb, J. B., Glover, G. H. & Heeger, D. J. Neuronal basis of contrast discrimination. *Vision Res* **39**, 257-269 (1999).

37 Legge, G. E. & Foley, J. M. Contrast masking in human vision. *J Opt Soc Am* **70**, 1458-1471 (1980).

38 Garcia-Perez, M. A. & Alcala-Quintana, R. Improving the estimation of psychometric functions in 2AFC discrimination tasks. *Frontiers in psychology* **2**, 96 (2011).

39 Kiani, R. & Shadlen, M. N. Representation of confidence associated with a decision by neurons in the parietal cortex. *Science* **324**, 759-764 (2009).

40 Garcia-Perez, M. A. & Alcala-Quintana, R. Shifts of the psychometric function: distinguishing bias from perceptual effects. *Quarterly journal of experimental psychology* **66**, 319-337 (2013).

41 Nienborg, H. & Macke, J. H. Using sequential dependencies in neural activity and behavior to dissect choice related activity in V2. in *Online Abstract Viewer.* (Society for Neuroscience, Washington, DC., 2014).

42 Schultz, W., Dayan, P. & Montague, P. R. A neural substrate of prediction and reward. *Science* **275**, 1593-1599 (1997).

43 Ding, L. & Gold, J. I. The basal ganglia's contributions to perceptual decision making. *Neuron* **79**, 640-649 (2013).

44 Lak, A. *et al.* Orbitofrontal cortex is required for optimal waiting based on decision confidence. *Neuron* **84**, 190-201 (2014).

45 Resulaj, A., Kiani, R., Wolpert, D. M. & Shadlen, M. N. Changes of mind in decision-making. *Nature* **461**, 263-266 (2009).

bioRxiv preprint doi: https://doi.org/10.1101/051912; this version posted May 6, 2016. The copyright holder for this preprint (which was not certified by peer review) is the author/funder, who has granted bioRxiv a license to display the preprint in perpetuity. It is made available under aCC-BY-NC-ND 4.0 International license.

Figures

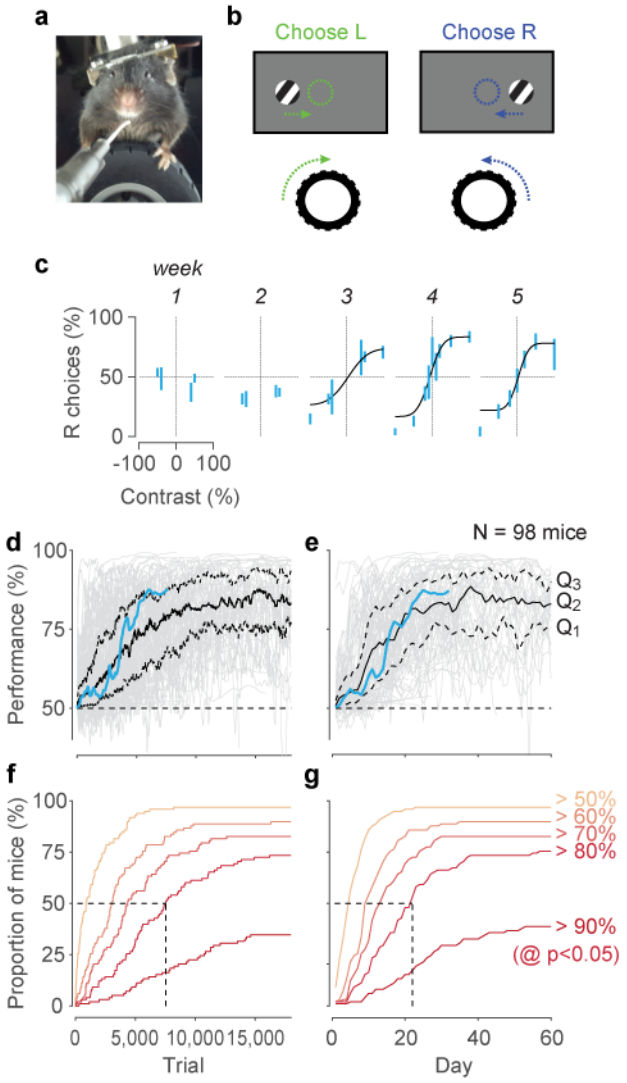

Figure 1. Fundamentals of the stimulus detection task, in its basic two-alternative forced-choice (2AFC) version. **a**. A typical setup showing the head-fixed mouse with forepaws on a steering wheel used to make choices. **b**. Schematic of the two possible stimulus conditions. At the onset, the grating is either on the left or on the right, and the mouse must turn the wheel (arrows) to move the grating to the final rewarded position (dashed circles). **c**. Psychometric data obtained in the first five weeks for an example mouse. Bars show the percentage of times the mouse chose the right stimulus (95% binomial confidence intervals), as a function of stimulus contrast. By convention we plot contrast of stimuli on the left as negative, and contrast on the right as positive. In later weeks, the data are fitted with a psychometric curve. **d**. Learning rates for a population of 98 mice. Performance is assessed on highly visible stimuli (≥40% contrast), as a function of number of trials. Blue trace highlights the example mouse in **c**. Gray traces indicate performance by individual mice, with black traces indicating the three quartiles: the median (Q2) and the 25th and 75th percentiles (Q1 and Q3). The approximate chance level is 50% (dashed line). These 98 mice were trained in the basic version of the task and in slight variations of the task. **e**. Same as **d** but expressed as a function of training days rather than trials. **f**. Cumulative probability curves showing the proportion of mice surpassing a given performance level as a function of trial number, with a significance level of $p<0.05$. **g**. Same as **f**, but expressed as a function of training days rather than trials.

bioRxiv preprint doi: https://doi.org/10.1101/051912; this version posted May 6, 2016. The copyright holder for this preprint (which was not certified by peer review) is the author/funder, who has granted bioRxiv a license to display the preprint in perpetuity. It is made available under aCC-BY-NC-ND 4.0 International license.

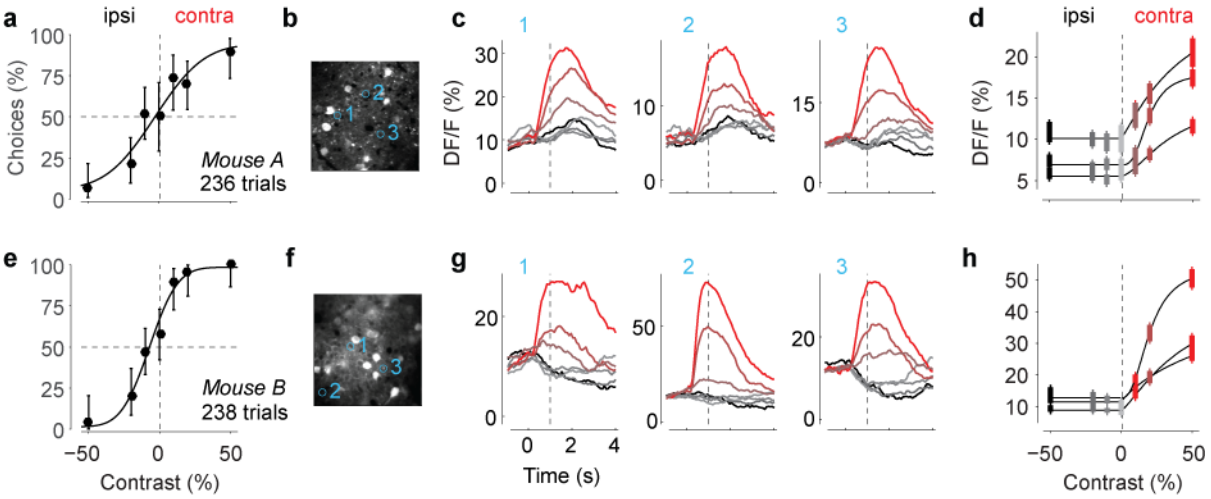

Figure 2. Imaging in V1 during the task. **a**. Psychometric curve for an example mouse, measured during two-photon imaging in area V1. **b.** Imaging field of view, with three cells (regions of interest) circled and numbered. **c**. Mean calcium activity averaged around the onset of the grating stimulus, grouped by stimulus condition (color codes are given in the next panel) for the three cells. Time zero denotes stimulus onset. Dashed line indicates the beginning of the interactive period, when the stimulus becomes movable (end of open loop). **d**. Response amplitudes of each cell as a function of stimulus contrast. Positive contrast denotes stimuli in the contralateral visual field, and negative contrast denotes stimuli in the ipsilateral visual field. Amplitude is mean response at 1 s after grating onset. Curves indicates fits of the function $p + qf(c)$, with $f(c)$ defined in Equation 1. Error bars indicate s.e.m. **e**-**h**. Same as **a**-**h**, for a different mouse.

bioRxiv preprint doi: https://doi.org/10.1101/051912; this version posted May 6, 2016. The copyright holder for this preprint (which was not certified by peer review) is the author/funder, who has granted bioRxiv a license to display the preprint in perpetuity. It is made available under aCC-BY-NC-ND 4.0 International license.

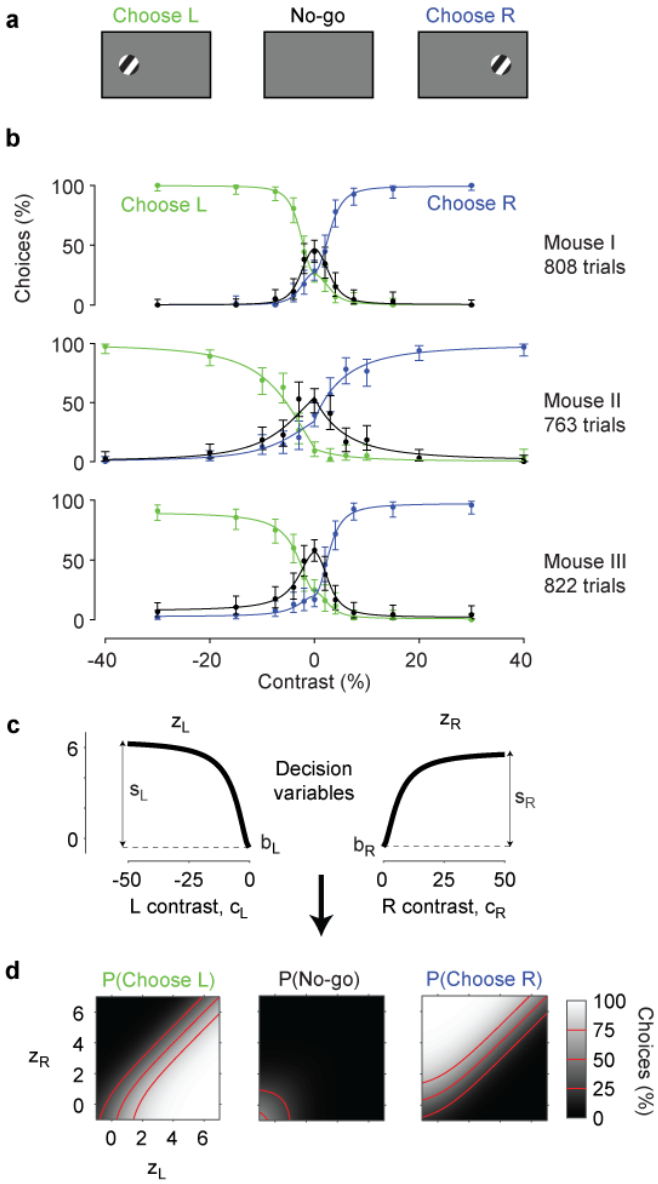

Figure 3. Elaboration of the stimulus detection task in a two-alternative unforced-choice (2AUC) version. **a**. In the 2AUC task, the mouse learns to choose left when the stimulus is on the left, choose right when the stimulus is on the right, and make neither response (No-go) if the stimulus is absent. **b.** Choices as a function of stimulus contrast and position for three sessions in three mice (rows). For each mouse the data show the proportion of left choices (green), right choices (blue), and no-go choices (black), as a function of stimulus contrast. As in all other plots, negative contrast denotes stimuli appearing on the left side. The data were fitted with the probabilistic observer model (smooth curves). Error bars are 95% binomial confidence intervals. **c**,**d**. Schematic of the model, with parameters obtained from the first mouse in **b**. The model defines two decision variables z_L and z_R, which grow with contrast presented on the left and on the right, respectively (**c**). These functions are each defined by two parameters, a bias *b* and a sensitivity *s*. The probability of each of the three possible choices depends uniquely on the two decision variables (**d**).

bioRxiv preprint doi: https://doi.org/10.1101/051912; this version posted May 6, 2016. The copyright holder for this preprint (which was not certified by peer review) is the author/funder, who has granted bioRxiv a license to display the preprint in perpetuity. It is made available under aCC-BY-NC-ND 4.0 International license.

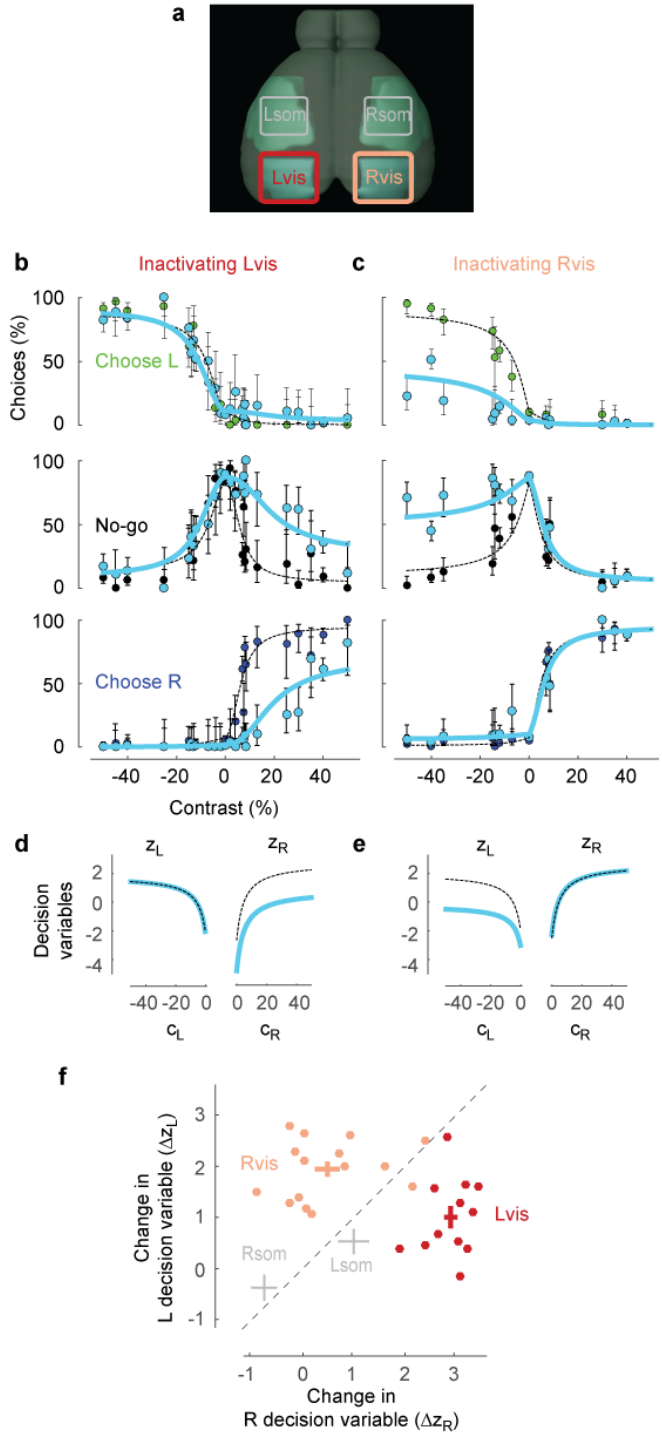

Figure 4. Effects of optogenetic inactivation of visual cortex. **a**. Map showing two regions inactivated in each hemisphere: left and right visual cortex (Lvis and Rvis, red and pink) and, as a control, left and right somatosensory cortex (Lsom and Rsom, gray). Optogenetic inactivation of these regions was performed in different sessions, in ~30% of the trials. **b**. Effects of inactivation of left visual cortex. Proportion of left, no-go, and right choices as a function of stimulus contrast, under control conditions (green, black, and blue dots) and during optogenetic inactivation (cyan dots). Curves indicate fits of the probabilistic model under control conditions (dashed) and during optogenetic inactivation (cyan). Error bars show 95% binomial confidence intervals. Data were obtained in 12 sessions (5,744 trials). **c**. Same as **b**, for inactivation of right visual cortex. Data were obtained in 15 sessions (7,619 trials). **d**. Decision variables obtained by the model fits in **b**, as a function of contrast on the left and right, in control condition (dashed) or during inactivation of left visual cortex (cyan). **e**. Same as **d**, for inactivation of right visual cortex. **f**. Summary of the effects of optogenetic inactivation in the four regions outlined in **a**. Effects are measured by the decrease in the left and right decision variables z_L or z_R at 50% contrast. Dots indicate individual sessions from two mice with inactivation of left visual cortex (red) or right visual cortex (pink). Crosses summarize the effects of inactivation in visual cortex (read and pink), and in somatosensory cortex (gray). The length of the crosses indicates ± s.e.m. in the two dimensions.

bioRxiv preprint doi: https://doi.org/10.1101/051912; this version posted May 6, 2016. The copyright holder for this preprint (which was not certified by peer review) is the author/funder, who has granted bioRxiv a license to display the preprint in perpetuity. It is made available under aCC-BY-NC-ND 4.0 International license.

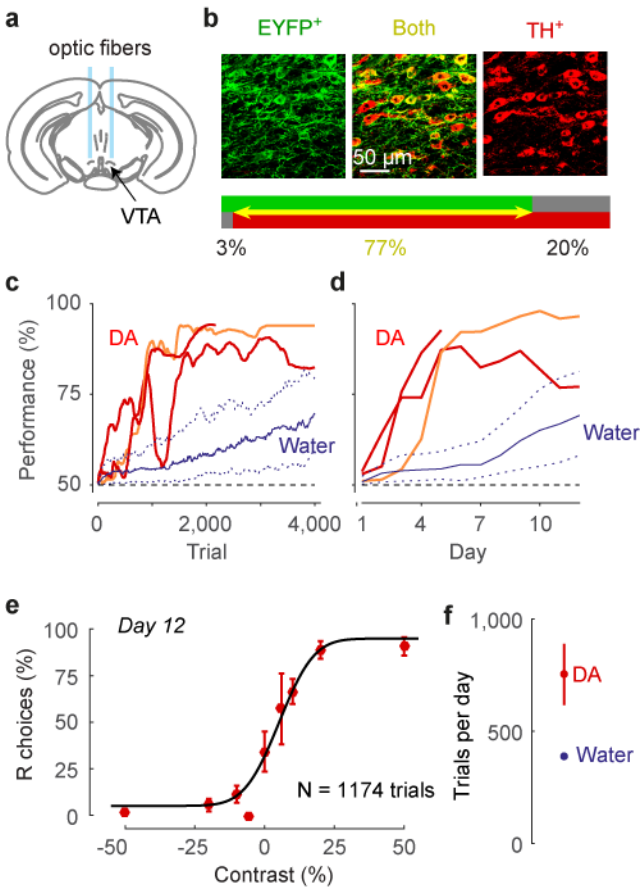

Figure 5. Using optogenetic phasic dopamine stimulation to train mice in the task. **a**. Schematic view of coronal section of the mouse brain (at Bregma -3.1 mm) showing ventral tegmental area (VTA), and fiber optics implanted above VTA to elicit release of dopamine (DA). **b**. Example images from a confocal microscope, showing expression of ChR2-EYFP (green) in TH+ (dopamine) neurons (red), and overlay showing both (yellow). The bars quantify the specificity of expression, showing statistics of ChR2-EYFP and TH+ expression in midbrain neurons (n = 763 neurons counted in 68 confocal images acquired from 4 mice). **c**,**d**. Rapid learning of the task in three mice receiving DA stimulation as a reward. Red and orange lines show rapid increase in the performance of naïve mice that were trained solely with optogenetic DA stimulation. For comparison, blue curves show results for mice that trained with water reward (median and quartile ranges, replotted from Figure 1). **e**. Psychometric function obtained from example animal (orange line in **c**,**d**) on the 12th day of behavioral training. Error bars show 95% binomial confidence intervals. **f**. Mean trials per day of mice receiving DA stimulation (red) compared to water rewards (blue). Error bars show s.e.m. (smaller than the dot for water rewards).

bioRxiv preprint doi: https://doi.org/10.1101/051912; this version posted May 6, 2016. The copyright holder for this preprint (which was not certified by peer review) is the author/funder, who has granted bioRxiv a license to display the preprint in perpetuity. It is made available under aCC-BY-NC-ND 4.0 International license.

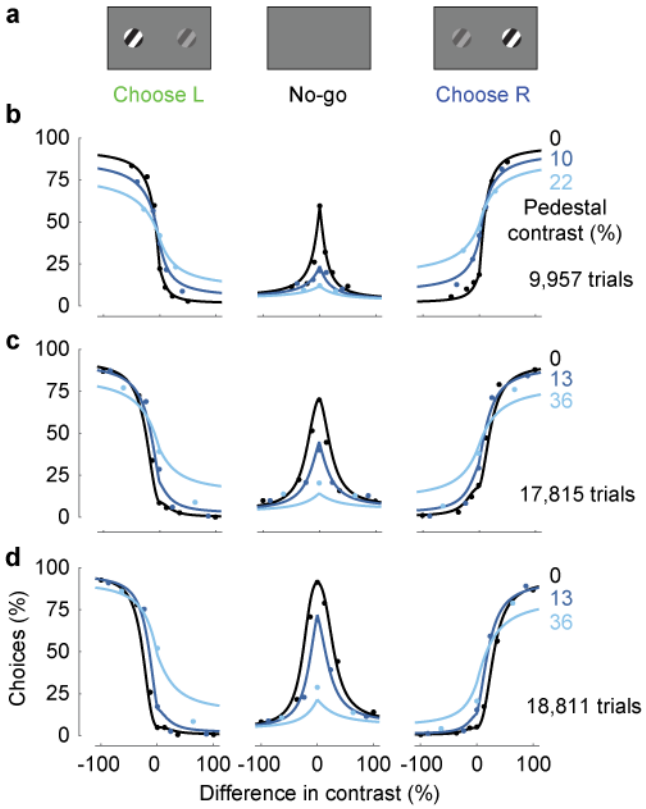

Figure 6. Extension of the 2AUC task to the study of contrast discrimination rather than detection. **a**. Schematic of the stimulus conditions used in the discrimination task. Gratings are presented on both sides and the mouse is rewarded for choosing the side with the highest contrast, or opting for no-go if both contrasts are zero. **b**. Psychometric data from 20 sessions in one mouse (9,957 trials). The three panels indicate, in the order, choices of the left stimulus, no-go, and choices of the right stimulus, as a function of the difference in contrast between the left and the right (c_R-c_L). The colors indicate the pedestal contrast, i.e. the minimum contrast present on the screen, min(c_L,c_R). **c**,**d**. Same as **b** for two more mice (27 sessions in each mouse, for a total of 17,815 trials in **c** and 18,811 trials in **d**).

bioRxiv preprint doi: https://doi.org/10.1101/051912; this version posted May 6, 2016. The copyright holder for this preprint (which was not certified by peer review) is the author/funder, who has granted bioRxiv a license to display the preprint in perpetuity. It is made available under aCC-BY-NC-ND 4.0 International license.

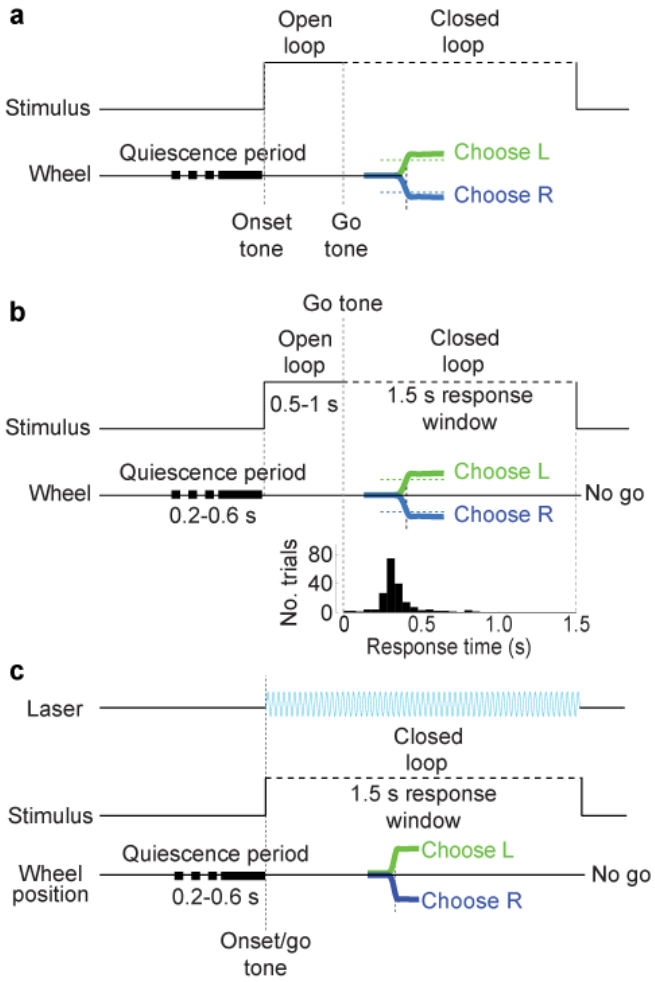

Supplementary Figure 1. Time courses of the basic 2AFC task and of some variants. **a**. Time course of the basic task. Mice start the trial by hold the wheel still (quiescence period). An onset tone may be played. The stimulus appears. Their position is initially fixed, i.e. it cannot be moved by moving the wheel (open loop period). After an optional "go tone", stimuli become paired with wheel position (closed loop). Choices are made when the stimulus reaches the center of the screen (in front of the mouse; rewarded choice) or an equal distance away from the onset position (incorrect choice). At this point a reward is given or a timeout with a noise stimulus. The experiments in Figure 2 employed a 2-3 s quiescence period, and a 1 s open loop period without a go tone. **b**. Time course of the 2AUC task shown in Figure 3. This variant included the go tone and also added a no-go choice option when the mouse did not response within the response window (rewarded on zero contrast trials). Histogram shows a typical distribution of response times in a session (time from go tone to completion of supra-threshold wheel turn). **c**. Time course of the 2AUC task for experiment in Figure 4. This variant did not include an open loop period. On ~33% of trials, stimuli were accompanied by laser illumination.

bioRxiv preprint doi: https://doi.org/10.1101/051912; this version posted May 6, 2016. The copyright holder for this preprint (which was not certified by peer review) is the author/funder, who has granted bioRxiv a license to display the preprint in perpetuity. It is made available under aCC-BY-NC-ND 4.0 International license.

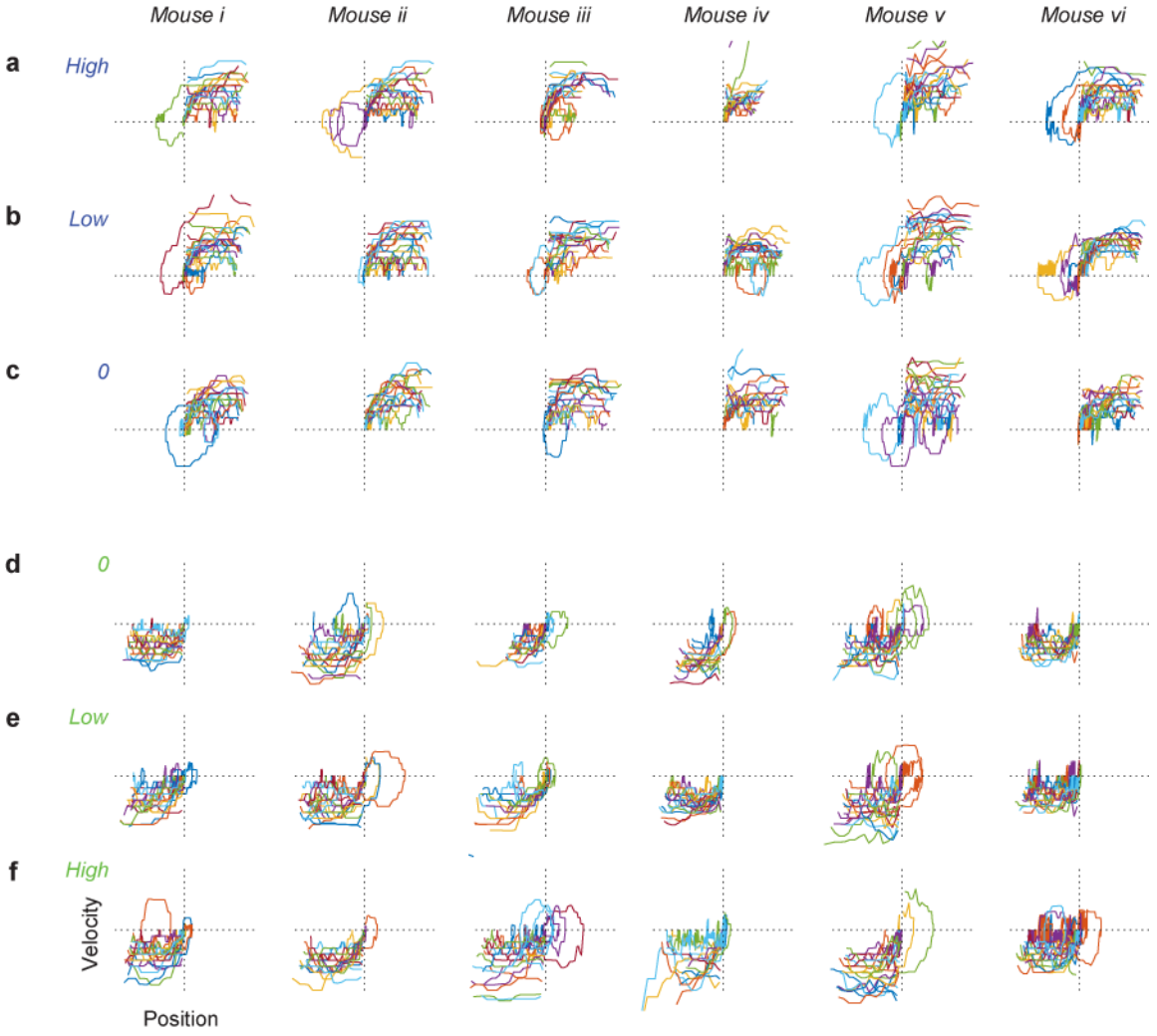

Supplementary Figure 2. Trajectories of wheel turns made by mice in response to stimuli. Traces show evolution of position and velocity during trajectories for turns made between stimulus onset and attainment of choice threshold. **a**-**c**: Trajectories that ended with a choice to the left, for stimuli that had high contrast on the left (a), low contrast on the left (b), or zero contrast (c). Any trials where the initial choice direction is inconsistent with the final choice must cross from one quadrant to the other (lower-left to upper-right), which is uncommon. **d**-**f**: Same as **a**-**c**, for trajectories that ended with a choice to the right.

bioRxiv preprint doi: https://doi.org/10.1101/051912; this version posted May 6, 2016. The copyright holder for this preprint (which was not certified by peer review) is the author/funder, who has granted bioRxiv a license to display the preprint in perpetuity. It is made available under aCC-BY-NC-ND 4.0 International license.

Supplementary Figure 3. Comparison of psychophysical performance in interactive trials vs. fixed-stimulus trials. These data were obtained in a single session in which two types of trial were randomly interleaved. In normal interactive trials, the steering wheel moved the stimulus (black). In the remaining trials, the mouse completes choices by turning the wheel as normal, but the stimulus remains fixed at the onset position (red). The ordinate plots the percentage of times the mouse chose the right stimulus, as a function of stimulus contrast. The psychometric curves fit across the two sets of trials (curves) are similar.

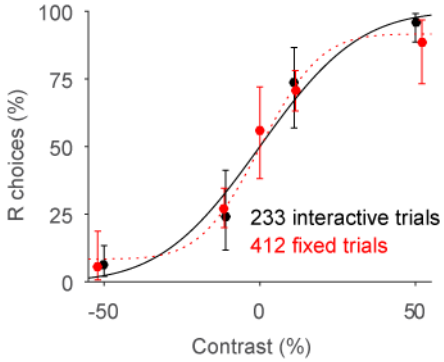

Supplementary Figure 4. Control electrophysiological measurements show optogenetic inactivation of visual cortex was spatially focused, with a radius of ~1 mm. We inserted multisite electrodes in visual cortex, and pooled responses from n = 110 single-unit and multiunit clusters with broad waveforms. We moved the laser at different distances from the electrode (abscissa) and measured the reduction in response relative to control response (modulation index, ordinate). The spot size and laser power (1.5 mW) were the same as in the behavioral experiments.

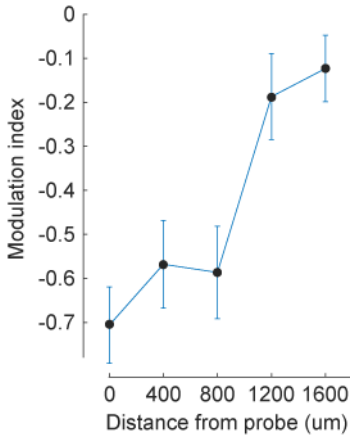

bioRxiv preprint doi: https://doi.org/10.1101/051912; this version posted May 6, 2016. The copyright holder for this preprint (which was not certified by peer review) is the author/funder, who has granted bioRxiv a license to display the preprint in perpetuity. It is made available under aCC-BY-NC-ND 4.0 International license.

Online Methods

All experiments were conducted according to the UK Animals Scientific Procedures Act (1986). Male and female mice between the ages of 8-24 weeks were used for all experiments. Mice were C57BL/6J or transgenics with a C57BL/6J background.

Head-plate implant

Mice were implanted with metal plate on the cranium to enable their heads to be fixed. To perform this surgery, mice were injected with an anti-inflammatory drug (4 mg/kg Carprofen subcutaneously) and anaesthetized using isoflurane (1–2%). Body temperature was maintained at 37°C using a heating pad and the eyes were protected with artificial tears to prevent drying (Viscotears). The head plate was implanted chronically by fixing it to the cranium with dental cement (Sun Medical). After surgery, mice were allowed at least 4 days to recover before water restriction and behavioral training began.

Training procedure

Most mice were trained using water as a reward. They were placed on a water restriction schedule in which they received a minimum daily amount (40 µL water per gram, daily mouse weight). Weight, behavior and general condition, were monitored for signs of dehydration.

Mice were then trained in a behavioral task, typically in daily one hour sessions over a period of weeks. On the first two training days, mice were head-fixed and trained for ~15 min to reduce stress during acclimatization. During the first few sessions mice were trained on a simplified version of the task, with 100% or 50% contrast, no inter-trial delays, quiescent period, or open loop period. Once they began to start reliably turning the wheel in both directions, the delays were increased to their final values. Once performance was reliably above chance level, lower contrasts were gradually introduced. Typically, mice were running on the final task parameters by week 2-3.

Task reward was also calibrated throughout the training process. When mice were naïve and did few trials they would be given more per correct trial (~3 µL), and as they became proficient and were completing 300 or more trials they would typically be given ~2 µL. If at the end of the behavioral session a mouse had not obtained their minimum daily fluid amount, the remaining fluid was provided later, in the home cage, in appropriately weighted Hydrogel packages. On rest days (typically, weekends) mice received their entire daily fluids through Hydrogel.

Task and stimulus control

The task was managed by custom MATLAB software. The response wheel was a Lego part with a rubber tire (with a flat 19 mm wide cross section and 31 mm in diameter). Its angle was measured using a rotary encoder (in most experiments, a Kübler 05.2400.1122.0100, with resolution: 0.9° or about 0.5 mm of wheel circumference) whose signal was acquired using a data acquisition device (National Instruments USB-6212). Specific volumes of water were dispensed by opening a solenoid valve (Neptune Research 161T011) for a calibrated duration of time.

Stimuli were presented on an LCD monitor (refresh rate 60 Hz) placed in front of the animal. Monitor luminance values for each color channel were linearized by using measurements from a photodiode. We used the Psychophysics Toolbox[46,47] to control graphics presentation for visual stimulation in MATLAB. The parameters used for Gabor textures were: standard deviations between 5-10°, wavelength 10°, horizontal or vertical orientations.

For each training session, the mouse was head-fixed in front of a computer screen with its forepaws resting upon a wheel. The mouse was able to turn the wheel with left or right movements of its forepaws. It was able to consume droplets of water dispensed via a spout close to its mouth, and a nearby speaker played auditory stimuli.

bioRxiv preprint doi: https://doi.org/10.1101/051912; this version posted May 6, 2016. The copyright holder for this preprint (which was not certified by peer review) is the author/funder, who has granted bioRxiv a license to display the preprint in perpetuity. It is made available under aCC-BY-NC-ND 4.0 International license.

On each trial, a target grating stimulus was initially presented on the left or the right of the screen. The grating was preceded by an auditory cue (100 ms before grating; 12 kHz pure tone lasting 100 ms with a 10 ms onset and offset ramp). Wheel turns by the mouse translated the grating horizontally: left turns moved the grating to the left; right turns moved the grating to the right. The mouse's goal was to bring the grating to the center of the screen, whereupon the grating would lock into place and the mouse received a reward. If instead the mouse translated the grating the same distance in the wrong direction, it would lock into place there (at the side of the screen) and a white noise sound was played for 2 s to indicate a timeout period. In either case, the grating remained locked in its response position for 1-2 s to remind the mouse of its action while it received its feedback, and then disappeared.

Eye tracking

On many sessions (typically imaging, inactivation, and some training sessions) we recorded eye position. We used a camera (DMK 21BU04.H, The Imaging Source) with a zoom lens (ThorLabs MVL7000) focused on the left or right eye of the mouse. We acquired videos of the eye with MATLAB's Image Acquisition Toolbox (MathWorks). We observed that eye movements were infrequent and predominately laterally directed away from a default resting position[48].

Dynamic estimate of task learning

We estimated task performance over learning using a state-space model which characterizes performance as the probability of a correct response as a function of trial number [49]. We applied this analysis to easier (contrast >= 40%) trials. Daily performance was estimated by taking the mean performance across each day's trials.

2AUC version

This version removes the auditory cue at stimulus onset, but the mouse was additionally required to be still for 0.5-1 s after stimulus onset which, once achieved, would be followed with an auditory go cue (12 kHz pure tone lasting 100 ms with a 10 ms onset and offset ramp; Supplementary Figure 1**b**). If the animal did not respond within 1.5 s of the go cue, this was considered a no-go response. No go responses were rewarded for blank stimuli trials or were met with a 2 s white noise burst for all other stimuli.

The multinomial logistic regression model was fit by maximum likelihood estimation. This was implemented either with MATLAB's inbuilt *fmincon* function or the *GLMNET* package [50]. The parameters c_{50} and n in Equation 1 were constrained to the ranges 0.01-0.8, and 0-3 respectively.

Responses in V1

We anaesthetized three 10-12 week old C57BL/6J female mice with isoflurane and implanted them with a metal head plate attached to the skull. We performed a 1 mm^2 craniotomy in the middle of a circular aperture in the head plate. The craniotomy was centered in the right primary visual cortex. We then injected them with GCaMP6m virus (AAV2/1-*syn*-GCaMP6m-WPRE, adeno-associated virus with human synapsin promoter driving expression of GCaMP6m, 50 nL undiluted $2x10^{13}$ genome copy/ml from Penn Vector Core; Ref. [51]) into the center of the craniotomy (stereotaxic coordinates 2.8 mm lateral and 3.3 mm caudal to Bregma) at a depth of 250 µm beneath the dura. We then covered the craniotomy with a two-layer glass coverslip construction, and sealed it with dental cement. The mice were allowed to recover for 1 week before water restriction and head-fixed training began.

Inactivation in visual cortex

Inactivation experiments were performed with transgenic mice expressing ChR2 in Pvalb-positive inhibitory interneurons (obtained by crossing a $Pvalb^{tm1(cre)Arbr}$ driver with an Ai32 reporter). Mice were prepared with a clear skull cap (similar to Ref. [32] but with UV-curing optical adhesive – ThorLabs NOA81 – instead of clear dental acrylic) and metal head plate for head-fixation. Light for inactivation was produced by a 473 nm diode laser (LuxX diode laser, Photon Lines Ltd) coupled to a fiber and collimated to a circle of approximately 1 mm diameter on the skull. Total laser power at the surface of the skull was about 1.5mW. The laser was targeted in stereotaxic coordinates

bioRxiv preprint doi: https://doi.org/10.1101/051912; this version posted May 6, 2016. The copyright holder for this preprint (which was not certified by peer review) is the author/funder, who has granted bioRxiv a license to display the preprint in perpetuity. It is made available under aCC-BY-NC-ND 4.0 International license.

relative to Bregma. Light was delivered as a 40Hz sinusoid beginning approximately synchronous with the visual stimulus onset and lasting until the mouse made a response. The task was the 2AUC detection variant, but responses could be made immediately upon stimulus onset. During individual sessions, inactivation was performed on approximately 30% of trials. One session out of 34 was excluded because performance on trials without laser inactivation was poor (max percent correct <50% for highest contrast stimuli on one side).

Optogenetic dopamine stimulation

We used DAT-Cre mice that were heterozygous for Cre recombinase under the control of DAT gene (B6.SJLSlc6a3tm1.1(cre)Bkmn/J, Jackson Laboratory) backcrossed with C57/BL6J mice. We injected 1 µL of diluted virus (AAV5.EF1a.DIO.hChr2(H134R)-eYFP.WPRE, 2.8×10^{12} unit/ml) into VTA and SNc (injection coordinates, from Bregma: AP = -3 mm, lateral: 0.5 mm and dorsal-ventral: 4.4 mm). An optic fiber was implanted over the same stereotaxic coordinate but with the fiber tips 0.5 mm above the virus injection site. The fiber and the head plate was secured using dental cement. We waited 3 weeks for virus expression before starting behavioral training. These mice had free access to food and water in their home cages and were trained in the 2AFC version of the task. In each trial, upon making a correct choice, animals received a short train of laser stimulation (473 nm, 12 pulses, pulse duration: 10 ms, inter pulse interval: 40 ms, laser power: 10-15 mW, measured at the tip of the fiber that was implanted in the brain) as well as a simultaneous sound click.

To quantify the specificity of ChR2 expression in dopamine neurons, animals were anesthetized (with sodium pentobarbitone) and perfused with 1X PBS followed by 4% formaldehyde in PBS. The brains were post-fixed in the same solution overnight and then kept in PBS containing 30% sucrose until settling. 50 µm coronal sections were collected and washed in PBS. Localization of fiber optic, DA cell bodies as well as ChR2-EYFP was confirmed using immunohistochemical methods. Sections were immunostained with antibodies to TH (New Market Scientific) and EYFP (Abcam) and secondary antibodies (Life Tech) labeled with Alexa Fluor 488 and 594, respectively. We quantified infection efficiency and specificity by counting cells (763 neurons) from 68 confocal images collected from 4 animals.

Contrast discrimination task

This task is based on the 2AUC task above, but gratings could be presented on both sides of the screen simultaneously, and the mice were rewarded for choosing (i.e. centering) the grating with the highest contrast, or rewarded 50% of the time if grating contrasts were equal. As in the 2AUC task, no response after 1.5 seconds was registered as a no-go response and rewarded only if no stimulus was present.

References

32 Guo, Z. V. *et al.* Flow of cortical activity underlying a tactile decision in mice. *Neuron* **81**, 179-194 (2014).
46 Pelli, D. G. The VideoToolbox software for visual psychophysics: Transforming numbers into movies. *Spatial Vision* **10**, 437-442 (1997).
47 Brainard, D. H. The Psychophysics Toolbox. *Spatial Vision* **10**, 433-436 (1997).
48 Ayaz, A., Saleem, A. B., Scholvinck, M. L. & Carandini, M. Locomotion controls spatial integration in mouse visual cortex. *Curr Biol* **23**, 890-894 (2013).
49 Smith, A. C. *et al.* Dynamic analysis of learning in behavioral experiments. *J Neurosci* **24**, 447-461 (2004).
50 Qian, J., Hastie, T., Friedman, J., Tibshirani, R. & Simon, N.Glmnet for Matlab. <www.stanford.edu/~hastie/glmnet_matlab/> (2013).
51 Chen, T. W. *et al.* Ultrasensitive fluorescent proteins for imaging neuronal activity. *Nature* **499**, 295-300 (2013).